# Magnetic properties of Lutetium and Yttrium doped $Ce_2Fe_{14}B$ magnets

Alex Bretaña,[1,*] Catherine Housley,[1] Henry Ajo,[1] Tucker Koenig,[1] Wenxia Li,[1] Benjamin S. Conner,[1] Patrick A. Ward,[1] Rosalie Greer,[1] Gregory Morrison,[2] Hans-Conrad zur Loye,[1,2] and Binod K. Rai[1]

[1] *Savannah River National Laboratory, Aiken, SC, 29808 USA*

[2] *Department of Chemistry and Biochemistry, University of South Carolina, 631 Sumter Street, Columbia, SC, USA*

(Dated: January 30, 2024)

The increasing demand for Nd-Dy and Sm-Co based permanent magnets is exacerbating the current critical materials shortage, therefore improving and optimizing current candidate critical element free permanent magnets is necessary to develop future clean energy technologies. In this work, we aim to increase the thermal stability and magnetic performance of $Ce_2Fe_{14}B$ based permanent magnets through the substitution of Ce ions with noncritical rare earth elements Lu and Y. The substitution of Lu (x=0, 0.05, 0.1, 0.15) for Ce ions in $(Lu_xCe_{2-x})Fe_{14}B$ was unsuccessful, likely due to disparities in ionic size and valencies, and failed to exhibit improved thermal stability or magnetic performance. In contrast, Y substitution for Ce ions in $(Y_xCe_{2-x})Fe_{14}B$ (x= 0.1, 0.2, 0.3, 0.4, 0.5) alloys was successful. Notably, these alloys demonstrated enhanced thermal stability, as evidenced by an increase in the Curie temperature, reaching a peak of 443 K at x= 0.5. Y substitution also helped to suppress the $CeFe_2$ Laves phase. Without loss of the anisotropy field Y substitution increased the saturation magnetization, $M_S$, peaking at $M_S = 125$ emu/g for a Y concentration of x= 0.4, demonstrating $(Y_{0.4}Ce_{1.6})Fe_{14}B$ as a potential critical element free permanent magnet with an energy product as high as 29 MGOe. This work is advantageous in developing low cost high performance permanent magnets with reduced or little to no critical rare earth elements.

## I. INTRODUCTION

Permanent magnets are integral components needed for future clean energy technologies, however the growing market for Nd-Dy and Sm-Co based permanent magnets is aggravating the scarcity of critical materials[1–7]. Designing, developing, and optimizing critical element free permanent magnets is essential for the future economy[8]. Based on $Nd_2Fe_{14}B$ permanent magnets, $Ce_2Fe_{14}B$ permanent magnets are an attractive low-cost alternative due to the highly abundant rare-earth Ce, however, $Ce_2Fe_{14}B$ displays several drawbacks, a rather low Curie temperature $T_C$ and a low magnetocrystalline anisotropy[5, 9]. In recent years, $Ce_2Fe_{14}B$ has seen a wealth of new studies being published in an attempt to improve these properties.

Chemical substitutions are an effective method to alter the magnetic properties of a permanent magnet, as seen in $Nd_2Fe_{14}B$ magnets[5, 10–14]. Recent studies have shown Co, La, Ni and Si substitutions in $Ce_2Fe_{14}B$ have been shown to improve or increase $T_C$, while Al and Hf have been shown to reduce it[15–19]. La and Co substitutions in $Ce_2Fe_{14}B$ have been shown to increase the saturation magnetization, $M_S$[15–17], while Al, Ni, and Si substitutions reduce $M_S$[18]. Hf, Ga, Ge, Ti, and Zr substitutions have been shown to slightly improve the magnetic properties through microstructure and grain refinement[19–23]. Despite Zr substitutions improving the magnetocrystalline anisotropy in other $R_2Fe_{14}B$ compounds[24, 25], Yin *et al.* determined Zr, as well as La, does not enhance the anisotropy in $Ce_2Fe_{14}B$[15]. Al, Ni, and Si substitutions have been shown to decrease magnetic anisotropy[18]. In a similar manner to Dy substitutions in $Nd_2Fe_{14}B$ magnets to improve coercivity and the thermodynamic properties, Y substitutions in $Nd_2Fe_{14}B$ and La substitutions in $Ce_2Fe_{14}B$ and $Y_2Fe_{14}B$ have both been shown to improve the coercivity and the thermodynamic properties[16, 17, 26–30]. These findings underscore the potential for tailored chemical substitutions to address specific challenges and advance the development of permanent magnets for sustainable energy solutions.

While chemical substitutions have proven effective in enhancing magnetic performance, the disproportionate reliance on costly rare-earth elements like Dy, Tb, Pr, and Nd contributes to price imbalances within the Rare Earth sector. In this work, the high abundant rare-earth Y and the heavier and rarer Lu are substituted for Ce in $Ce_2Fe_{14}B$ in an attempt to improve the magnetic and thermodynamic properties similar to Dy in $Nd_2Fe_{14}B$ based permanent magnets. To evaluate the performance of such substitutions, a comprehensive characterization of the magnetic properties of $(Lu_xCe_{2-x})Fe_{14}B$ (x=0, 0.05, 0.1, 0.15) and $(Y_xCe_{2-x})Fe_{14}B$ (x=0.1, 0.2, 0.3, 0.4, 0.5) alloys was carried out. We confirmed the successful incorporation of Y into the $Ce_2Fe_{14}B$ phase whereas the attempt to substitute Lu in $Ce_2Fe_{14}B$ was unsuccessful, most likely, due to the disparities in ionic size and valencies between Lu and Ce. The efficacy of Y substitutions in $Ce_2Fe_{14}B$ was evident through observed changes in lattice parameters, Curie temperatures, and magnetization measurements. Conversely, Lu substitutions in $Ce_2Fe_{14}B$ did not manifest any discernible alterations in these properties.

* alex.bretana@srnl.doe.gov

## II. EXPERIMENTAL DETAILS

The alloys with nominal compositions of $(Lu_xCe_{2-x})Fe_{14}B$ (x=0.05, 0.1, 0.15) and $(Y_xCe_{2-x})Fe_{14}B$ (x=0.1, 0.2, 0.3, 0.4, 0.5) were synthesized by conventional arc melting in an argon atmosphere. The starting materials are Ce (Ames Laboratory and Thermo Scientific, 99.8%), Fe (Alfa Aesar, 99.99%), B (Thermo Scientific, 99.4%), Y (Ames Laboratory), and Lu (Ames Laboratory). The starting materials in the appropriate compositions were arc melted in an electric arc furnace and remelted at least 4 to 5 times to ensure a homogeneous ingot. The ingot was then sealed in a quartz tube under vacuum and the ampoule was annealed in a box furnace at 900°C for 14 days then quenched in ice water. The phase of as melted and annealed ingots was characterized by room temperature X-ray diffraction (XRD) using a Bruker D8 Advance diffractometer with monochromated Cu $K_{\alpha 1}$ radiation. Microstructure and surface analysis was characterized using a Carl Zeiss Sigma VP field emission scanning electron microscope and elemental dispersive X-ray spectroscopy (EDS) was measured using an Oxford Instruments X-Max 20 silicon drift detector.

The magnetic properties of the alloys were measured by a Quantum Design Magnetic Property Measurement System 3 (MPMS3). The anisotropic magnetization was measured at room temperature on polycrystalline pieces that were ground in a pestle and mortar and aligned inside a gel capsule using a similar procedure as described by Sales *et al.*[31]. The magnetic transition temperatures of the $(Y_xCe_{2-x})Fe_{14}B$ (x=0.1, 0.2, 0.3, 0.4, 0.5) alloys were obtained by differential scanning calorimetry (DSC) while the $(Lu_xCe_{2-x})Fe_{14}B$ (x=0.05, 0.1, 0.15) alloys were obtained using a thermogravimetric analyzer (TGA) with a strong permanent magnet positioned directly above the sample. Upon reaching the Curie temperature, the force exerted on the sample by the strong permanent magnet vanishes and a visible mass change is observed.

## III. RESULTS AND DISCUSSION

XRD on as melted and annealed $(Lu_xCe_{2-x})Fe_{14}B$ (x=0.05, 0.1, 0.15) alloys determined Lu substitution increased the volume fraction of the $\alpha$-Fe impurity phase while also suppressing the $CeFe_2$ Laves phase. As melted alloys consisted primarily of $Ce_2Fe_{14}B$ and $\alpha$-Fe phases with an occasional small fraction of $CeFe_2$ phase that could barely be resolved by XRD measurements. Upon annealing, stoichiometric $Ce_2Fe_{14}B$ and all Lu doped alloys except x=0.15 consisted of primarily $Ce_2Fe_{14}B$ phase with a small fraction of $\alpha$-Fe impurity as seen in Fig. 1, while x=0.15 had a second impurity which consisted of a very small amount of $Ce_2O_3$[32]. The lattice parameters for $Ce_2Fe_{14}B$ (x=0) as determined by Rietveld refinement are $a = b = 8.75(1)$Å and $c = 12.10(2)$Å, as seen in the middle panel of Fig. 2 and in agreement with previous reports[15].

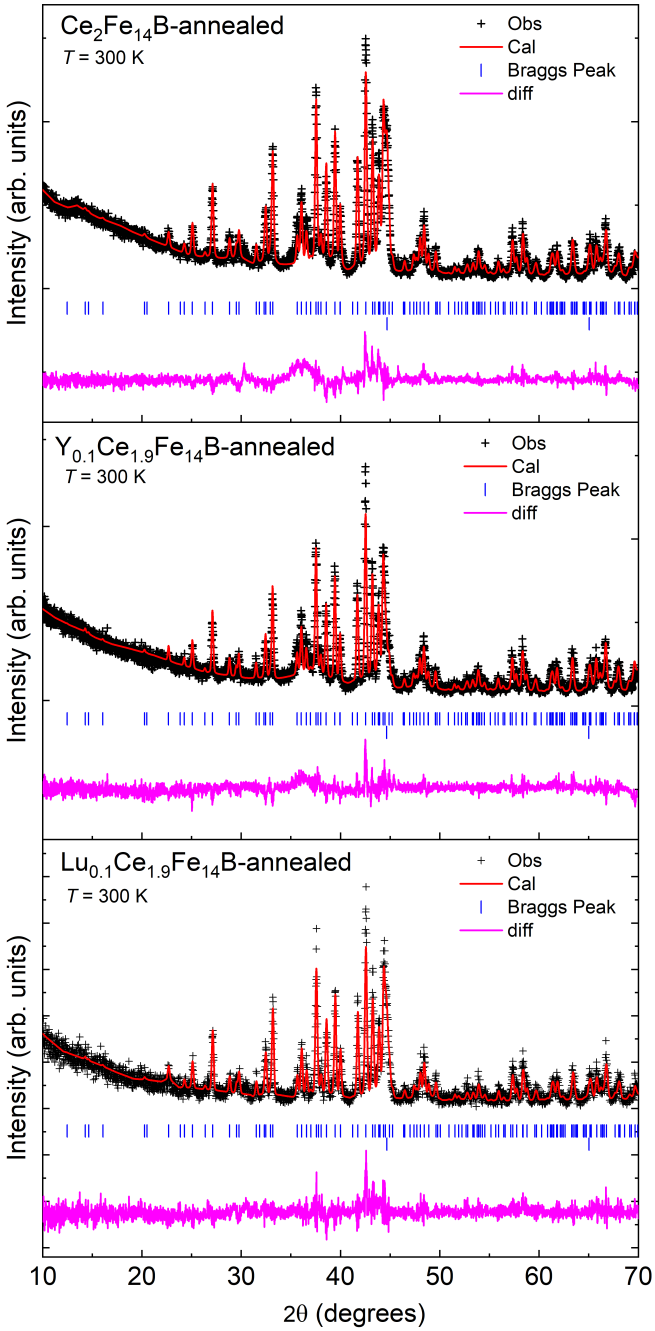


FIG. 1. Rietveld Refinement of room temperature XRD data for annealed $Ce_2Fe_{14}B$ (top panel), $(Y_{0.1}Ce_{1.9})Fe_{14}B$ (middle panel), and $(Lu_{0.1}Ce_{1.90})Fe_{14}B$ (bottom panel) alloys. All annealed alloys plotted are composed primarily of $Ce_2Fe_{14}B$ phase with small $\alpha$-Fe impurities. Vertical blue ticks correspond to the position of the calculated Bragg peaks of all phases (from top to bottom, 2-14-1 and $\alpha$-Fe).

EDS on as melted $(Lu_xCe_{2-x})Fe_{14}B$ (x=0.05, 0.1, 0.15) alloys determined an average of 0.98(0.33)% (atomic percent) Lu concentration in the $Ce_2Fe_{14}B$ phase for x=

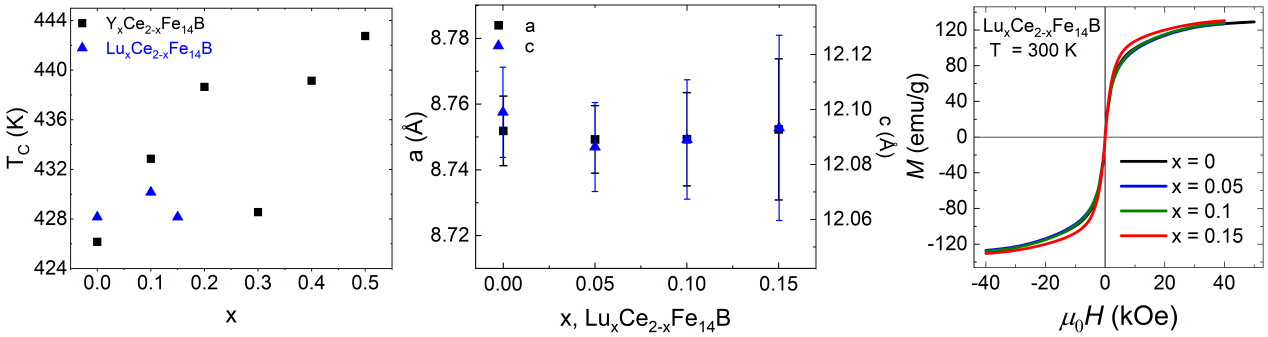


FIG. 2. (Left Panel) Curie temperatures as determined by DSC and TGA for annealed $Ce_2Fe_{14}B$ , $(Lu_xCe_{2-x})Fe_{14}B$ (x=0.05, 0.1, 0.15), and $(Y_xCe_{2-x})Fe_{14}B$ (x=0.1, 0.2, 0.3, 0.4, 0.5) alloys. (Middle Panel) Lattice parameters as determined by Reitveld refinement of room temperature XRD data for annealed $Ce_2Fe_{14}B$ and $(Lu_xCe_{2-x})Fe_{14}B$ (x=0.05, 0.1, 0.15) alloys. (Right panel) Isotropic magnetization vs field measurements taken at room temperature for annealed $Ce_2Fe_{14}B$ and $(Lu_xCe_{2-x})Fe_{14}B$ (x=0.05, 0.1, 0.15) alloys.

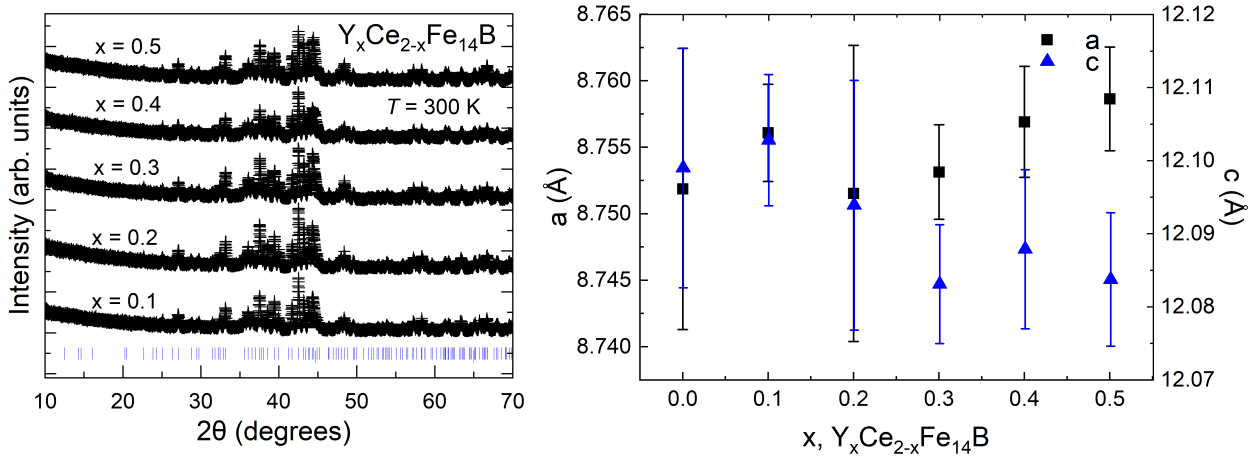


FIG. 3. (Left Panel) Raw room temperature XRD data for annealed $(Y_xCe_{2-x})Fe_{14}B$ (x=0.1, 0.2, 0.3, 0.4, 0.5) alloys. (Right Panel) Lattice parameters as determined by Reitveld refinement of room temperature XRD data for annealed $Ce_2Fe_{14}B$ and $Y_2Fe_{14}B$ (x=0.1, 0.2, 0.3, 0.4, 0.5) alloys.

0.15, while for x= 0.1, Lu concentration was found to be 0.60(0.15)%, and undetectable in EDS for x= 0 (resolution of EDS is ∼0.5% atomic percent). Upon annealing, no Lu concentration was observed in the $Ce_2Fe_{14}B$ phase in EDS. In all annealed samples, the lack of Lu concentration in the $Ce_2Fe_{14}B$ phase was further confirmed through isothermal magnetization measurements, as seen in the right panel of Fig. 2, which revealed little to no change in saturation magnetization, $M_S$, and again through TGA measurements, as seen in the left panel of Fig. 2, showing little to no change in $T_C$ regardless of Lu concentration x.

We attributed the instability associated with Lu substitution in $Ce_2Fe_{14}B$ to be due to two factors, the size of the Lu ions in comparison to Ce, as well as the mixed valency of Ce in $Ce_2Fe_{14}B$ [9]. $Ce^{3+}$ ion's radius is 102 pm whereas $Lu^{3+}$ ion's radius is 86 pm[33]. Alam *et al.* determined the instability in Ce substitution in $(Ce_xNd_{2-x})Fe_{14}B$ at concentrations larger than x= 0.5 is due to a 15 − 20% difference in volumes between $Nd_2Fe_{14}B$ and $Ce_2Fe_{14}B$ , as well as the differences in Nd and Ce valences[34]. In $Ce_2Fe_{14}B$ , Ce has a mixed valence state of 3.44, a mixture of $Ce^{3+}$ and $Ce^{4+}$ states, known as the mixed valence $\alpha$-state[24]. Lutetium can be found in various oxidation states from +0 to +3, however Lu does not form a +4 oxidation state due to its complete $4f$ shell. This difference in size and oxidation preference potentially lead Lu to segregate out of the $Ce_2Fe_{14}B$ phase upon heat treatment.

XRD on as melted and annealed $(Y_xCe_{2-x})Fe_{14}B$ (x=0.1, 0.2, 0.3, 0.4, 0.5) determined Y substitution also increased the volume fraction of the $\alpha$-Fe impurity phase while suppressing the $CeFe_2$ Laves phase. As with Lu substitution, as melted alloys of $(Y_xCe_{2-x})Fe_{14}B$ (x=0.1, 0.2, 0.3, 0.4, 0.5) consisted of primarily $Ce_2Fe_{14}B$ and $\alpha$-Fe phases with an occasional small fraction of $CeFe_2$ phase that could barely be resolved by XRD measurements. Upon annealing, all Y substituted alloys con-

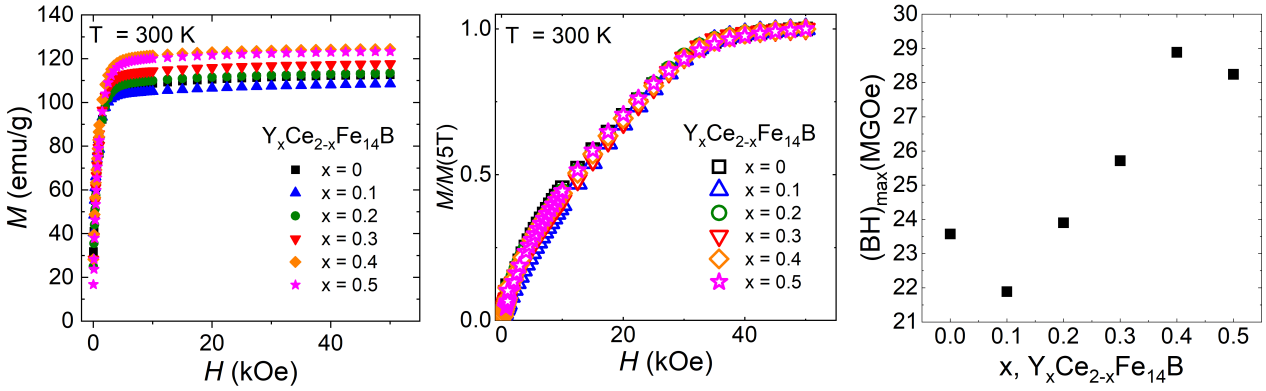


FIG. 4. (Left Panel) Field dependent magnetization measurements on aligned powder with the magnetic field applied along the easy direction for annealed $Ce_2Fe_{14}B$ and $(Y_xCe_{2-x})Fe_{14}B$ (x=0.1, 0.2, 0.3, 0.4, 0.5) alloys. (Middle Panel) Field dependent magnetization measurements on aligned powder with the magnetic field applied along the hard direction for annealed $Ce_2Fe_{14}B$ and $(Y_xCe_{2-x})Fe_{14}B$ (x=0.1, 0.2, 0.3, 0.4, 0.5) alloys. (Right Panel) The estimated energy product of $Ce_2Fe_{14}B$ and $(Y_xCe_{2-x})Fe_{14}B$ (x=0.1, 0.2, 0.3, 0.4, 0.5) alloys calculated using the saturation magnetization, reveals $(Y_{0.4}Ce_{1.6})Fe_{14}B$ as a potential critical material free permanent magnet with an energy product as high as 29 MGOe.

sisted of primarily $Ce_2Fe_{14}B$ phase with a small fraction of $\alpha$-Fe impurity as seen in Fig. 1. As can be seen in the right panel of Fig. 3, there is little to no change in the $a$-axis with small concentrations of Y up to x=0.3, as expected as the $a$ axis of $Y_2Fe_{14}B$ is very similar to that of $Ce_2Fe_{14}B$ [29]. However, increasing the Y concentration to x= 0.4 and higher, Rietveld refinements determined a very small increase along the $a$-axis to 8.758(4)Å at x=0.5. Along the $c$-axis, we see a shrinkage with increasing Y concentration to 12.083(9)Å at x= 0.5 associated with the smaller size of Y ions replacing Ce ions[33]. EDS measurements confirmed Y substitution for Ce ions at the appropriate concentrations in the $Ce_2Fe_{14}B$ phase for all annealed alloys; for example, at x= 0.1, Y concentration was found to be 0.68(0.04)% (atomic percent), close to the expected percentage, 0.625%.

As can be seen in the left panel of Fig. 2, the Curie temperature increases with increasing Y concentration reaching a maximum of nearly 443 K at the maximum Y concentration doped in this study, x= 0.5. At the lowest level of Y concentration studied, x= 0.1, field dependent magnetization measurements at room temperature revealed a slight decrease in saturation magnetization, $M_S$, however with increasing Y concentration, we see an increase in $M_S$ above that of $Ce_2Fe_{14}B$ ($M_S$ = 113 emu/g). At the highest Y concentration studied, x= 0.5, $M_S$ = 123 emu/g, albeit at x= 0.4, $M_S$ peaks at the highest value seen in this study of 125 emu/g, as shown in the left panel of Fig. 4. The field dependence of magnetically aligned powder samples with the magnetic field applied along the hard direction can be seen in the middle panel of Fig. 4, as can be seen, we observe little to no change with increasing Y concentration. Thus, without loss of the anisotropy field, Y substitution improves the thermal stability of of $Ce_2Fe_{14}B$ phase by increasing the Curie temperature, while simultaneously increasing the saturation magnetization, $M_S$. Estimating the energy product using $M_S$ (80% of $(M_S)^2/4$), reveals $(Y_{0.4}Ce_{1.6})Fe_{14}B$ as a potential critical element free permanent magnet with an energy product as high as 29 MGOe, as can be seen in the right panel of Fig. 4.

## IV. CONCLUSION

We synthesized and characterized $(Lu_xCe_{2-x})Fe_{14}B$ (x=0, 0.05, 0.1, 0.15) and $(Y_xCe_{2-x})Fe_{14}B$ (x=0.1, 0.2, 0.3, 0.4, 0.5) to systemically evaluate their performance as critical element free permanent magnets. We determined Lu did not successfully substitute for Ce ions in $Ce_2Fe_{14}B$ , potentially due to the difference in ionic size and valencies between Lu and Ce, however Y substitution was successful. With increasing Y concentration, we see a small increase along the $a$-axis to 8.758(4)Å and a slight shrinkage along the c−axis 12.083(9)Å at x= 0.5. In addition, Y also increased the thermal stability of $Ce_2Fe_{14}B$ through an increase in Curie temperatures up to a maximum of 443 K at x= 0.5. Without loss of the anisotropy field, at x= 0.1, Y substitution reduced the saturation magnetization, $M_S$, however with increasing Y concentration, $M_S$ increases and peaks at $M_S$ = 125 emu/g for a Y concentration of x= 0.4. Estimating the energy product using the saturation magnetization, reveals $(Y_{0.4}Ce_{1.6})Fe_{14}B$ as a potential critical element free permanent magnet with an energy product as high as 29 MGOe. Our experimental results highlight the benefits of Y substitution in improving the thermal stability and magnetic performance of $Ce_2Fe_{14}B$ based permanent magnets.

## V. ACKNOWLEDGMENTS

This work was supported by the Laboratory Directed Research and Development (LDRD) program within the Savannah River National Laboratory (SRNL). This work was produced by Battelle Savannah River Alliance, LLC under Contract No. 89303321CEM000080 with the U.S. Department of Energy. Publisher acknowledges the U.S. Government license to provide public access under the DOE Public Access Plan (http://energy.gov/downloads/doe-public-access-plan).

[1] Masato Sagawa, Setsuo Fujimura, Norio Togawa, Hitoshi Yamamoto, and Yutaka Matsuura. New material for permanent magnets on a base of nd and fe. *Journal of Applied Physics*, 55(6):2083–2087, 1984.

[2] John J Croat, Jan F Herbst, Robert W Lee, and Frederick E Pinkerton. Pr-fe and nd-fe-based materials: A new class of high-performance permanent magnets. *Journal of Applied Physics*, 55(6):2078–2082, 1984.

[3] JMD Coey. Hard magnetic materials: A perspective. *IEEE Transactions on magnetics*, 47(12):4671–4681, 2011.

[4] S Sugimoto. Current status and recent topics of rare-earth permanent magnets. *Journal of Physics D: Applied Physics*, 44(6):064001, 2011.

[5] JF Herbst. $R_2fe_{14}b$ materials: Intrinsic properties and technological aspects. *Reviews of Modern Physics*, 63(4): 819, 1991.

[6] BK Rai and SR Mishra. Magnetically enhanced hard–soft $smco_5$–feni composites obtained via high energy ball milling and heat treatment. *Journal of magnetism and magnetic materials*, 344:211–216, 2013.

[7] M Lamichanne, BK Rai, SR Mishra, VV Nguyen, and JP Liu. Magnetic properties hard-soft $smco_5$-feni and $smco_5$-feco composites prepared by electroless coating. *Open J. Compos. Mater*, 2:119–124, 2012.

[8] Jun Cui, Matthew Kramer, Lin Zhou, Fei Liu, Alexander Gabay, George Hadjipanayis, Balamurugan Balasubramanian, and David Sellmyer. Current progress and future challenges in rare-earth-free permanent magnets. *Acta Materialia*, 158:118–137, 2018.

[9] JF Herbst and WB Yelon. Crystal and magnetic structure of $ce_2fe_{14}b$ and $lu_2fe_{14}b$. *Journal of magnetism and magnetic materials*, 54:570–572, 1986.

[10] D Goll and Helmunt Kronmüller. High-performance permanent magnets. *Naturwissenschaften*, 87:423–438, 2000.

[11] Josef Fidler and Thomas Schrefl. Overview of nd–fe–b magnets and coercivity. *Journal of Applied Physics*, 79 (8):5029–5034, 1996.

[12] Michael A Susner, Benjamin S Conner, Bayrammurad I Saparov, Michael A McGuire, Ethan J Crumlin, Gabriel M Veith, Huibo Cao, Kavungal V Shanavas, David S Parker, Bryan C Chakoumakos, et al. Flux growth and characterization of ce-substituted $nd_2fe_{14}b$ single crystals. *Journal of Magnetism and Magnetic Materials*, 434:1–9, 2017.

[13] S Pandian, V Chandrasekaran, G Markandeyulu, KJL Iyer, and KVS Rama Rao. Effect of co, dy and ga on the magnetic properties and the microstructure of powder metallurgically processed nd–fe–b magnets. *Journal of alloys and compounds*, 364(1-2):295–303, 2004.

[14] Gérard Delette. $Nd_2fe_{14}b$ permanent magnets substituted with non-critical light rare earth elements (ce, la): A review. *Journal of Magnetism and Magnetic Materials*, page 170768, 2023.

[15] Li Yin, Jiaqiang Yan, Brian C Sales, and David S Parker. Critical-element-free permanent-magnet materials based on $ce_2fe_{14}b$. *Physical Review Applied*, 17(6):064020, 2022.

[16] Ming Zhang, Zhubai Li, Baogen Shen, Fengxia Hu, and Jirong Sun. Permanent magnetic properties of rapidly quenched $(la, ce)_2fe_{14}b$ nanomaterials based on la–ce mischmetal. *Journal of Alloys and Compounds*, 651:144–148, 2015.

[17] Jiasheng Zhang, Xuefeng Liao, Qing Zhou, Ke Xu, Wenbin Fan, Hongya Yu, Xichun Zhong, and Zhongwu Liu. Enhanced hard-magnetic properties and thermal stability of nanocrystalline ce-rich ce-fe-b alloys by combining la substitution and si addition. *Journal of Magnetism and Magnetic Materials*, 552:169217, 2022.

[18] Kayode Orimoloye, Dominic H Ryan, Frederick E Pinkerton, and Mamoun Medraj. Intrinsic magnetic properties of $ce_2fe_{14}b$ modified by al, ni, or si. *Applied Sciences*, 8 (2):205, 2018.

[19] Qingzheng Jiang, Minglong Zhong, Qichen Quan, Weikai Lei, Qingwen Zeng, Yongfeng Hu, Yaping Xu, Xianjun Hu, Lili Zhang, Renhui Liu, et al. Magnetic properties and microstructure of melt-spun $ce_{17}fe78 - xb_6hf_x$ (x= 0–1.0) alloys. *Journal of Magnetism and Magnetic Materials*, 444:344–348, 2017.

[20] BJ Ni, H Xu, XH Tan, and XL Hou. Study on magnetic properties of $ce_{17}fe_{78-x}zr_xb_6$ (x= 0–2.0) alloys. *Journal of Magnetism and Magnetic Materials*, 401:784–787, 2016.

[21] Changquan Zhou, Minxiang Pan, Qiong Wu, and Hangfu Yang. Improvement of magnetic properties for ti doped ce-fe-b alloys: Effectively inhibiting $cefe_2$ phase formation. *Journal of Magnetism and Magnetic Materials*, 502: 166564, 2020.

[22] Sajjad Ur Rehman, Qingzheng Jiang, Kai Liu, Lunke He, Han Ouyang, Lili Zhang, Lei Wang, Shengcan Ma, and Zhenchen Zhong. Phase constituents, magnetic properties, intergranular exchange interactions and transition temperatures of ge-doped cefeb alloys. *Journal of Physics and Chemistry of Solids*, 132:182–186, 2019.

[23] Ren-Quan Wang, Xin Shen, Ying Liu, and Jun Li. Effects of ga addition on the formability of main phase and microstructure of hot-deformed ce–fe–b magnets. *IEEE Transactions on Magnetics*, 52(9):1–6, 2016.

[24] TW Capehart, RK Mishra, and FE Pinkerton. Determination of the zirconium site in zirconium-substituted $nd_2fe_{14}b$. *Journal of applied physics*, 73(10):6476–6478, 1993.

[25] M Jurczyk and WE Wallace. Magnetic behavior of $r_{1.9}zr_{0.1}fe_{14}b$ and $r_{1.9}zr_{0.1}fe_{12}co_2b$ compounds. *Journal of magnetism and magnetic materials*, 59(3-4): L182–L184, 1986.

[26] A Handstein, J Schneider, K-H Müller, R Krewenka, R Grössinger, and HR Kirchmayr. Temperature dependence of magnetic properties of sintered nd-fe-b magnets modified with dy. *Journal of magnetism and magnetic materials*, 83(1-3):199–200, 1990.

[27] W Chen, JM Luo, YW Guan, YL Huang, M Chen, and YH Hou. Grain boundary diffusion of dy films prepared by magnetron sputtering for sintered nd–fe–b magnets. *Journal of Physics D: Applied Physics*, 51(18):185001, 2018.

[28] Xiaodong Fan, Kan Chen, Shuai Guo, Renjie Chen, Don Lee, Aru Yan, and Caiyin You. Core–shell y-substituted nd–ce–fe–b sintered magnets with enhanced coercivity and good thermal stability. *Applied Physics Letters*, 110 (17), 2017.

[29] Xuefeng Liao, Jiasheng Zhang, Hongya Yu, Xichun Zhong, Abdul Jabbar Khan, Xuan Zhou, Hui Zhang, and Zhongwu Liu. Exceptional elevated temperature behavior of nanocrystalline stoichiometric $y_2fe_{14}b$ alloys with la or ce substitutions. *Journal of Materials Science*, 54 (23):14577–14587, 2019.

[30] Zhongwu Liu, Dongyan Qian, and Dechang Zeng. Reducing dy content by y substitution in nanocomposite ndfeb alloys with enhanced magnetic properties and thermal stability. *IEEE transactions on magnetics*, 48(11): 2797–2799, 2012.

[31] Brian C Sales, Bayrammurad Saparov, Michael A McGuire, David J Singh, and David S Parker. Ferromagnetism of $fe_3sn$ and alloys. *Scientific reports*, 4(1): 7024, 2014.

[32] QM Lu, J Niu, WQ Liu, M Yue, and Z Altounian. Enhanced magnetic properties of spark plasma sintered (la/ce)–fe–b magnets. *IEEE Transactions on Magnetics*, 53(11):1–3, 2017.

[33] Alexander Frank Wells. *Structural inorganic chemistry*. Oxford Classic Texts in the Ph, 2012.

[34] Aftab Alam, Mahmud Khan, R William McCallum, and Duane D Johnson. Site-preference and valency for rare-earth sites in $(r\text{-}ce)_2fe_{14}b$ magnets. *Applied Physics Letters*, 102(4), 2013.